Current Research in Toxicology 6 (2024) 100155

Contents lists available at ScienceDirect

Current Research in Toxicology

journal homepage: www.journals.elsevier.com/current-research-in-toxicology

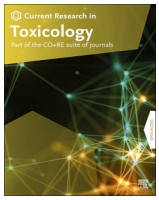

Roles of oxidative stress/JNK/ERK signals in paraquat-triggered hepatic apoptosis

Kuan-I Lee [a,1], Kai-Min Fang [b,1], Chun-Ying Kuo [c,1], Chun-Fa Huang [d,e], Shing-Hwa Liu [f], Jui-Ming Liu [g], Wei-Cheng Lai [a], Kai-Chih Chang [h], Chin-Chuan Su [c,i,*], Ya-Wen Chen [j,*]

[a] Department of Emergency, Taichung Tzu Chi Hospital, Buddhist Tzu Chi Medical Foundation, Taichung 427, Taiwan
[b] Department of Otolaryngology, Far Eastern Memorial Hospital, New Taipei City 220, Taiwan
[c] Department of Otorhinolaryngology, Head and Neck Surgery, Changhua Christian Hospital, Changhua County 500, Taiwan
[d] School of Chinese Medicine, College of Chinese Medicine, China Medical University, Taichung 404, Taiwan
[e] Department of Nursing, College of Medical and Health Science, Asia University, Taichung 413, Taiwan
[f] Institute of Toxicology, College of Medicine, National Taiwan University, Taipei 100, Taiwan
[g] Department of Urology, Taoyuan General Hospital, Ministry of Health and Welfare, Taoyuan 330, Taiwan
[h] Center for Digestive Medicine, Department of Internal Medicine, China Medical University Hospital, Taichung 404, Taiwan
[i] Department of Post-Baccalaureate Medicine, College of Medicine, National Chung Hsing University, Taichung 402, Taiwan
[j] Department of Physiology, School of Medicine, College of Medicine, China Medical University, Taichung 404, Taiwan

ARTICLE INFO

Keywords:
Paraquat
Hepatotoxicity
Apoptosis
Oxidative stress
JNK
ERK1/2

ABSTRACT

Paraquat (PQ), a toxic and nonselective bipyridyl herbicide, is one of the most extensively used pesticides in agricultural countries. In addition to pneumotoxicity, the liver is an important target organ for PQ poisoning in humans. However, the mechanism of PQ in hepatotoxicity remains unclear. In this study, we found that exposure of rat hepatic H4IIE cells to PQ (0.1–2 mM) induced significant cytotoxicity and apoptosis, which was accompanied by mitochondria-dependent apoptotic signals, including loss of mitochondrial membrane potential (MMP), cytosolic cytochrome *c* release, and changes in the Bcl-2/Bax mRNA ratio. Moreover, PQ (0.5 mM) exposure markedly induced JNK and ERK1/2 activation, but not p38-MAPK. Blockade of JNK and ERK1/2 signaling by pretreatment with the specific pharmacological inhibitors SP600125 and PD98059, respectively, effectively prevented PQ-induced cytotoxicity, mitochondrial dysfunction, and apoptotic events. Additionally, PQ exposure stimulated significant oxidative stress-related signals, including reactive oxygen species (ROS) generation and intracellular glutathione (GSH) depletion, which could be reversed by the antioxidant *N*-Acetylcysteine (NAC). Buffering the oxidative stress response with NAC also effectively abrogated PQ-induced hepatotoxicity, MMP loss, apoptosis, and phosphorylation of JNK and ERK1/2 protein, however, the JNK or ERK inhibitors did not suppress ROS generation in PQ-treated cells. Collectively, these results demonstrate that PQ exposure induces hepatic cell toxicity and death via an oxidative stress-dependent JNK/ERK activation-mediated downstream mitochondria-regulated apoptotic pathway.

1. Introduction

Paraquat (PQ; 1,1′-dimethyl-4,4′-bipyridium dichloride), an important bipyridinium herbicide, is widely used worldwide to control broad-leaved weeds and grasses in crop land and aquatic areas. The herbicidal activity of PQ involves inhibition of the reduction of $NADP^+$ to nicotinamide adenine dinucleotide phosphate (NADPH) during photosynthesis and interference with intracellular electron transfer *via* reactive

Abbreviations: ERK, extracellular signal-regulated kinase; GSH, glutathione; JNK, c-Jun N-terminal kinase; MMP, mitochondrial membrane potential; MAPKs, mitogen-activated protein kinases; NAC, *N*-acetylcysteine; NADPH, nicotinamide adenine dinucleotide phosphate; PARP, poly(ADP-ribose) polymerase; PQ, paraquat; ROS, reactive oxygen species.

* Corresponding authorsat: Department of Physiology, School of Medicine, College of Medicine, China Medical University, Taichung 404, Taiwan (Y.-W. Chen); Department of Otorhinolaryngology, Head and Neck Surgery, Changhua Christian Hospital, Changhua County 500, Taiwan (C.-C. Su).

E-mail addresses: 91334@cch.org.tw (C.-C. Su), ywc@mail.cmu.edu.tw (Y.-W. Chen).

[1] These authors contributed equally to this study.

https://doi.org/10.1016/j.crtox.2024.100155
Received 21 October 2023; Received in revised form 18 January 2024; Accepted 7 February 2024
Available online 10 February 2024

oxygen species (ROS) induction (Awadalla, 2012). Noteworthy, PQ is classified among the most poisonous herbicides with high water solubility as it enters runoff, leading to water and environmental pollution (Moustakas et al., 2016). Moreover, regular exposure to PQ may cause occupational hazards, especially for workers in agricultural areas (Cantor and Young-Holt, 2002; Dalvie et al., 1999). Many clinical deaths have been reported owing to PQ intoxication through random or optional consumption (such as accidents or suicide attempts, respectively), which is considered to induce strong pneumotoxicity (Isha et al., 2018; Liu et al., 2019). Similar to the lungs, the liver is a hallmark target organ of systemic PQ poisoning (Hong et al., 2000; Spangenberg et al., 2012). Epidemiological and animal experimental data have shown hepatotoxic characteristics (including abnormal liver function and pathological liver injury) after PQ exposure in humans and mammals (Almeida et al., 2021; Deveci et al., 1999; Hong et al., 2000; Takegoshi et al., 1988). However, few studies have investigated the molecular mechanisms underlying the toxicological effects of PQ in the liver.

PQ is categorized as a possible (Class C) carcinogen, while its toxicity is molecularly related to redox cycling and generation of massive toxic ROS and subsequent induction of oxidative injuries (U.S. Environmental Protection Agency's Integrated Risk Information System (IRIS)). Several studies have also found that PQ (0.1–1 mM) can be reduced to an unstable radical that is then reoxidized to form a cation and generate a superoxide anion and hydroxyl free radical, leading to mammalian cell damage and death (such as fibroblasts, lymphocytes, neuronal cells, and pulmonary epithelial cells) (Alural et al., 2015; Jimenez Del Rio and Velez-Pardo, 2008; Wu et al., 2023). The liver is major site for detoxification and xenobiotic metabolism, and has the potential to easily produce excess ROS, thus posing a high risk for chemical-induced oxidative damage (Li et al., 2015; Zeinvand-Lorestani et al., 2018). Therefore, the liver has been suggested as a major target for PQ poisoning. In experimental animals, histopathological alterations, oxidative stress damage marker expressions (such as GSH depletion and lipidperoxidation production), and apoptosis in the liver were observed after administration of PQ (El-Boghdady et al., 2017; Semeniuk et al., 2021; Shi et al., 2015).

Furthermore, mitogen-activated protein kinase (MAPK) family, a class of serine/threonine protein kinases that are widely expressed in mammalian cells, including c-Jun N-terminal kinase (JNK), extracellular signal-regulated kinase (ERK)1/2, and p38-MAPK, is crucial for the maintenance and/or regulation of cellular processes, including cell survival and apoptosis (Sun et al., 2015). Many studies have demonstrated that exposure to chemical stimuli or toxic pollutants can induce excessive ROS production, causing mammalian cell damage and death, accompanied by MAPKs activation-regulated apoptosis pathway (Fu et al., 2020; Huang et al., 2018). For example, the ROS-MAPK signaling pathway is involved in the pathophysiological states of liver diseases and injuries (such as alcoholic- and nonalcoholic-fatty liver disease, and drug-induced hepatotoxicity) (Song et al., 2016; Win et al., 2018). Moreover, the results from *in vivo* and in vitro models showed that PQ exposure induced ROS production-triggered apoptosis in neuronal cells and lung epithelial cells, but not in hepatocytes, via the IRE1/ASK1/JNK cascade-mediated pathway, JNK1/Parkin-mediated mitophagy, or ERK/MAPK-associated signaling pathway (Shen et al., 2017; Sun et al., 2018; Yang et al., 2009; Zhang et al., 2019). Although PQ poisoning-induced liver injury has been reported (El-Boghdady et al., 2017; Sharifi-Rigi et al., 2019), the action mechanisms underlying PQ-induced ROS production in hepatotoxicity have not yet been clarified.

Collectively, in this study, we investigated how PQ influences the regulated apoptotic pathways of MAPKs and contributes to hepatocyte death. Moreover, we investigated whether oxidative stress plays a crucial role in PQ-induced hepatotoxicity and whether it mediates the abovementioned apoptotic pathways.

2. Materials and Methods

2.1. Materials

Unless otherwise specified, all chemicals (including PQ) and laboratory plastic ware were purchased from Sigma-Aldrich (St. Louis, MO, USA) and Falcon Labware (Becton, Dickinson and Company, Franklin Lakes, NJ, USA), respectively. Dulbecco's modified Eagle's medium (DMEM), fetal bovine serum (FBS), and antibiotics (penicillin–streptomycin (Cat. No.: 15140122), and gentamicin (Cat. No.: 15710064)) were purchased from Gibco/Invitrogen (Thermo Fisher Scientific, Waltham, MA, USA). Mouse- or rabbit- monoclonal antibodies specific to cleaved caspase-3 (Cat. No.: #9661), cleaved caspase-7 (Cat. No.: #9491), PARP (Cat. No.: #9542), cytochrome *c* (Cat. No.: #11940), phosphorylated (p)-JNK (Cat. No.: #9255), p-ERK1/2 (Cat. No.: #4377), p-p38 (Cat. No.: #9216), JNK-1 (Cat. No.: #3708), ERK1/2 (Cat. No.: #9102), p38 (Cat. No.: #8690), and β-actin (Cat. No.: #8457), and secondary antibodies [horseradish peroxidase (HRP)-conjugated anti-mouse IgG (Cat. No.: #7076) or anti-rabbit IgG (Cat. No.: #7074) were purchased from Cell Signaling Technology (Danvers, MA, USA).

2.2. Rat hepatic H4IIE cell culture

Rat hepatic H4IIE cells were purchased from American Type Culture Collection (CRL-1548, American Type Culture Collection, Manassas, VA, USA), and cultured in a humidified chamber with a 5 % CO_2-95 % air mixture at 37 °C and maintained in DMEM containing glucose (4.5 g/L) and L-glutamine (2 mmol/L) supplemented with 10 % FBS and antibiotics (1 % penicillin–streptomycin and 0.5 % gentamicin).

2.3. Measurement of cell viability

H4IIE cells were washed with fresh media and cultured in 96-well plates (2×10^4 cells/well) and then treated with PQ (0.1–2 mM) in the absence or presence of SP600125 (20 μM), PD98059 (20 μM), or NAC (3 mM) prior to treatment with PQ for 24 h. After incubation, the medium was aspirated and cells were incubated with fresh medium containing 0.2 mg/mL 3-(4, 5-dimethyl thiazol-2-yl-)-2, 5-diphenyl tetrazolium bromide (MTT). After 4 h incubation at 37 °C, the medium was removed and the blue formazan crystals were dissolved in 100 μL dimethyl sulfoxide (DMSO). Absorbance at 570 nm was measured using an enzyme-linked immunosorbent assay microplate reader (Biotek μQuant Monochromatic Microplate Spectrophometer, MTX Lab Systems, Inc.).

2.4. Measurement of Caspase-3 activity

H4IIE cells were seeded (2×10^5 cells/well) in 24-well culture plates and treated with PQ (0.25–1 mM) in the absence or presence of 20 μM Z-DEVD-FMK, 20 μM SP600125, 20 μM PD98059, or 3 mM NAC (prior to treatment with PQ) at 37 °C. At the end of the treatments (for 24 h), the cell lysates were incubated at 37 °C with 10 μM Ac-DEVD-AMC, a caspase-3/CPP32 substrate (Promega Corporation, Madison, WI, USA), for 1 h. The fluorescence of the cleaved substrate was measured using a spectrofluorometer (Gemini XPS Microplate Reader, Molecular Devices, San Jose, CA, USA) at excitation and emission wavelengths of 380 and 460 nm, respectively.

2.5. Determination of mitochondrial membrane potential

Mitochondrial membrane potential (MMP) was analyzed using the $DiOC_6$ fluorescent probe, which is a positively charged mitochondria-specific fluorophore. Briefly, H4IIE cells were seeded (2×10^5 cells/well) in 24-well culture plates and treated with 0.5 mM PQ in the absence or presence of SP600125 (20 μM), PD98059 (20 μM), or NAC (3 mM) (prior to treatment with PQ) for 24 h. At the end of the treatments,

the cells were incubated with medium containing 100 nM $DiOC_6$ for 30 min at 37 °C. After incubation with the dye, the cells were harvested, washed twice with phosphate buffered saline (PBS), and then re-suspended in ice-cold PBS. The MMP was determine using a flow cytometer (excitation at 475 nm and emission at 525 nm; FACSCalibur, Becton Dickinson, Sunnyvale, CA, USA).

2.6. Determination of ROS production

ROS generation was monitored by flow cytometry using the peroxide-sensitive fluorescent probe: 2′, 7′-dichlorofluorescein diacetate (DCFH-DA, Molecular Probes, Inc, Eugene, OR, USA), as described by Fu et al.(2020). Briefly, cells were seeded at 2×10^5 cells/well in a 24-well plate and treated with 0.5 mM PQ in the absence or presence of 3 mM NAC (prior to treatment with PQ). At the end of the treatments, cells were incubated with medium containing 20 μM DCFH-DA for 15 min at 37 °C. After incubation with the dye, the cells were resuspended in ice-cold PBS and placed on ice in the dark. The intracellular peroxide levels were measured using a flow cytometer (FACScalibur, Becton Dickinson and Company, USA), with emitted a fluorescent signal at 525 nm.

2.7. Analysis of intracellular glutathione (GSH) content

H4IIE cells were seeded at 2×10^5 cells/well in a 24-well plate and incubated with PQ in the absence or presence of NAC (3 mM) (prior to treatment with PQ). At the end of the treatments (for 8 h), cells were incubated in a medium containing 60 μM monochlorobimane (mBCL, a fluorescent probe for determining intracellular GSH levels) for a further 30 min at 37 ℃. After loading the cells with mBCL, the supernatant was discarded, and cells were washed twice with PBS and then lysed in lysis buffer (10 mM Tris, 0.25 M sucrose in 0.05 % Triton X-100, pH 7.5). The mBCL-GSH related fluorescence intensity of the intracellular fraction was monitored using a Gemini XPS microplate reader (Molecular Devices, USA) at excitation and emission wavelengths of 385 and 485 nm, respectively.

2.8. Western blot analysis

Western blotting was performed using standard protocols as previously described (Huang et al., 2021). H4IIE cells were seeded at 1×10^6 cells/well in a 6-well culture plate and treated with PQ (0.5 mM) in the presence or absence of SP600125 (20 μM), PD98059 (20 μM), or NAC (3 mM) (prior to treatment with PQ). At the end of various time-course treatments, the cells were washed with PBS and Protein Extraction Solution (iNtRON Biotechnology, Gyeonggi-do, Korea) was added. The protein concentration was determined using a bicinchoninic acid protein assay kit (Pierce, Rockford, IL, USA). Equal amounts of proteins (50 μg per lane) were subjected to electrophoresis on 10 % (w/v) SDS-polyacrylamide gel and transferred onto polyvinylidene difluoride (PVDF) membranes. The membranes were blocked for 1 h in PBST (PBS with 0.05 % Tween-20) containing 5 % nonfat dry milk. After blocking, the membranes were incubated with the specific antibodies against caspase-3, −7, PARP, p-JNK, p-ERK1/2, p-p38, JNK, ERK1/2, p38, and β-actin in 0.1 % PBST (1:1000) for 12–16 h at 4 ℃. After three additional washes in 0.1 % PBST (15 min each), the respective HRP-conjugated secondary antibodies were applied (in 0.1 % PBST (1:2500)) for 1 h at 4 ℃. The antibody-reactive bands were detected by enhanced chemiluminescence reagents (Pierce™, Thermo Fisher Scientific Inc., USA) and analyzed using a luminescent image analyzer (ImageQuant™ LAS-4000; GE Healthcare Bio-Sciences, Corp., Piscataway, NJ, USA). For the detection of cytosolic cytochrome *c* expression levels, the cells were detached, washed twice with PBS, and then homogenized with a pestle and mortar in extraction buffer [0.4 M mannitol, 25 mM MOPS (pH 7.8), 1 mM EGTA, 8 mM cysteine, and 0.1 % (w/v) bovine serum albumin]. Cell debris was removed by centrifugation at 6,000 × *g* for 2 min. The supernatant was centrifuged at 12,000 × *g* for 15 min to pellet the mitochondria. Cytochrome *c* levels in the supernatant (cytosolic fraction) were detected using western blot analysis.

2.9. Real-time quantitative RT-PCR analysis

The expression of apoptosis-related genes was evaluated using real time quantitative RT-PCR (qPCR) as previously described (Lu et al., 2011). Briefly, intracellular total RNA was extracted from the liver tissue using RNeasy kits (Qiagen, Hilden, Germany) and reverse transcribed into cDNA using the AMV RTase (reverse transcriptase enzyme; Promega Corporation, Madison, WI, USA) according to the manufacturer's instructions. Each sample (2 μL cDNA) was then tested with Real-Time SYBR Green PCR reagent (Invitrogen, USA) with rat specific primers as follows: Bcl-2, forward: 5′-GCTACGAGTGGGATACTGG-3′ and reverse: 5′- GTGTGCAGATGCCGGTTCA-3′ (Dinh et al., 2008); Bax, forward: 5′-CTGCAGAGGATGATTGCTGA-3′ and reverse: 5′-GATCAGCTCGGGCACTTTAG-3′ (Dinh et al., 2008); β-actin, forward: 5′-CGTTGACATCCGTAAAGACC-3′ and reverse: 5′- AGCCACCAATCCACACAGAG-3′ (Dinh et al., 2008); in a 25-μL reaction volume, and amplification was performed using an ABI StepOnePlus™ Sequence Detection System (Applied Biosystems, Thermo Fisher Scientific, Inc.). Cycling conditions were 10 min of polymerase activation at 95 °C followed by 40 cycles at 95 °C for 15 s and 60 °C for 60 s. Real-time fluorescence detection was performed during the 60 °C annealing/extension step of each cycle. Melt-curve analysis was performed on each primer set to ensure that no primer dimers or nonspecific amplifications were present under the optimized cycling conditions. After 40 cycles, data analysis was performed using StepOne™ software version 2.1 (Applied Biosystems, Thermo Fisher Scientific, Inc.). All amplification curves were analyzed with a normalized reporter (R_n: the ratio of the fluorescence emission intensity to the fluorescence signal of the passive reference dye) threshold of 0.2 to obtain the C_T values (threshold cycle). The reference control genes were measured with four replicates in each PCR run, and their average C_T was used for relative quantification analyses (Pfaffl et al., 2002). TF expression data were normalized by subtracting the mean of reference gene C_T value from their C_T value (ΔC_T). The Fold Change value was calculated using the expression $2_T^{-\Delta\Delta C}$, where $\Delta\Delta C_T$ represents $\Delta C_{T\text{-condition of interest}} - \Delta C_{T\text{-control}}$. Prior to conducting statistical analyses, the fold change from the mean of the control group was calculated for each individual sample.

2.10. Statistical analysis

Data are presented as means ± standard error (SE.) of at least three independent experiments. All data analyses were performed using SPSS software version 12.0 (SPSS, Inc., Chicago, IL, USA). For each experimental test condition, the significant difference compared to the respective controls was assessed by one-way or two-way analysis of variance (ANOVA) followed by Tukey's post hoc test. The p value of less than 0.05 was considered a significant difference.

3. Results

3.1. PQ induces apoptotic cell death in hepatic H4IIE cells

To examine PQ-induced hepatocyte damage, we investigated the cytotoxic effects of PQ on cultured H4IIE cells. Treating H4IIE cells with PQ for 24 h significantly reduced the number of viable cells in a concentration dependent manner (0.1 mM, 86.9 ± 2.4 % of control; 0.25 mM, 62.4 ± 2.6 % of control; 0.5 mM, 49.2 ± 1.4 % of control; 1 mM, 39.9 ± 1.2 % of control; 2 mM, 31.8 ± 1.0 % of control; $p < 0.05$) (Fig. 1A).

Next, we investigated whether apoptosis was involved in PQ-induced hepatocyte damage. We analyzed caspase-3 activity, a characteristic biomarker of apoptosis. As shown in Fig. 1B, H4IIE cells treated with PQ for 24 h showed a significant increase in caspase-3 activity (0.25 mM,

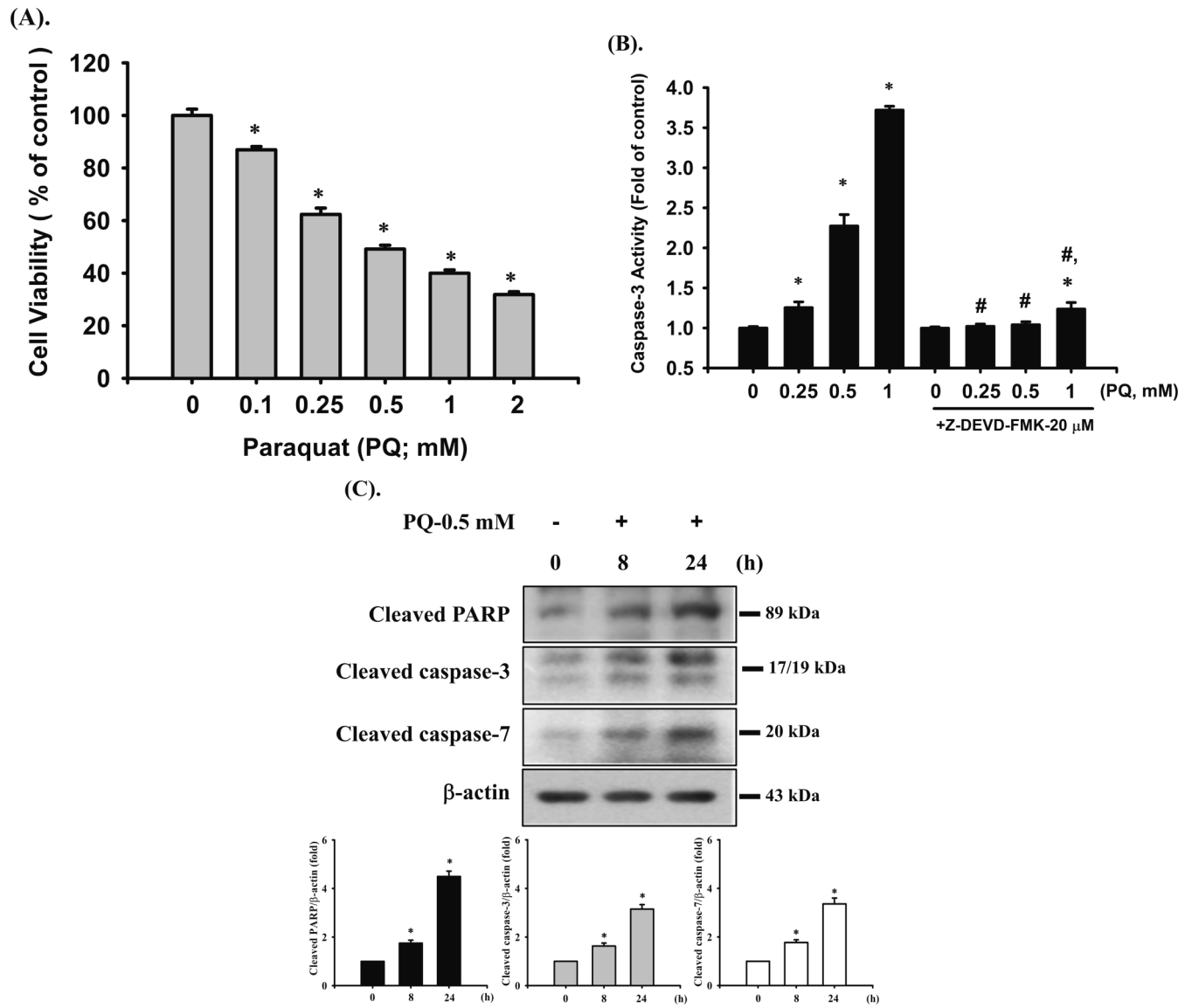

Fig. 1. Paraquat (PQ) induced cytotoxicity by apoptosis in H4IIE cells. (A) H4IIE cells were cultured and treated with PQ (0.1–2 mM) for 24 h, and cell viability was determined using the MTT assay. (B) Cells were treated with PQ (0.25–1 mM) in the absence or presence of Z-DEVD-FMK (20 μM, a specific caspase 3 inhibitor), and caspase-3 activity was examined using the CaspACE^{TM} fluorometric activity assay kit. (C) H4IIE cells were treated with PQ (0.5 mM) for 8 and 24 h, and the cleavage form of PARP and caspase-3 and -7 were examined by western blotting as described in the Materials and Methods section. Data in A and B are presented as mean ± S. E. for six independent experiments with triplicate determination. $^{*}p < 0.05$ compared to the vehicle control. $^{\#}p < 0.05$ compared to PQ treatment alone. Results shown in C are representative images of at least three independent experiments, and β-actin was used as a loading control.

1.25 ± 0.14 fold of control; 0.5 mM, 2.27 ± 0.32 fold of control; 1 mM, 3.72 ± 0.12 fold of control; $p < 0.05$) relative to the untreated control group, which could be effectively prevented by pretreatment with 20 μM Z-DEVD-FMK (a specific caspase-3 inhibitor). Based on these findings, the median effective concentration (EC_{50}) of PQ for cell viability and caspase-3 activity in H4IIE cells was approximately 0.5 mM. This concentration was therefore used in subsequent experiments.

Western blot analysis also showed a marked increase in the protein expression of the cleaved forms of PARP and caspase-3 and -7 in PQ (0.5 mM)-treated H4IIE cells (Fig. 1C). These results suggest that PQ-induced hepatocyte death is mainly due to apoptosis.

3.2. *Pq-induced apoptosis is mediated by an intrinsic mitochondria-dependent pathway in H4IIE cells*

To further elucidate whether PQ-induced apoptosis in hepatocytes was mediated by a mitochondria-dependent pathway, the effects of PQ on MMP (by flow cytometry using the mitochondrial cationic dye $DiOC_6$) and cytochrome *c* release (by western blot analysis) were analyzed. As shown in Fig. 2A, treatment of H4IIE cells with 0.5 mM PQ for 8 h revealed a slight, but statistically significant loss of MMP (89.9 ± 2.8 % of control; $p < 0.05$) and induced greater depolarization of MMP (55.9 ± 3.9 % of control; $p < 0.05$) after 16 and 24 h treatments. Cytochrome *c* release from mitochondria into the cytosolic fraction slightly increased after treatment of cells with 0.5 mM PQ for 8 h, and it dramatically increased after 16 and 24 h of treatment (Fig. 2B). In addition, changes in the gene expression levels of the Bcl-2 family members were investigated. As shown in Fig. 2C, treatment of H4IIE cells with 0.5 mM PQ (for 8 and 24 h) markedly decreased *Bcl-2* (anti-apoptotic) and increased *Bax* (pro-apoptotic) mRNA expression levels, which led to a significant shift in the anti-apoptotic/pro-apoptotic ratio toward a state associated with apoptosis. These results indicate that an intrinsic mitochondria-dependent apoptotic pathway plays an important role in PQ-induced hepatocyte death.

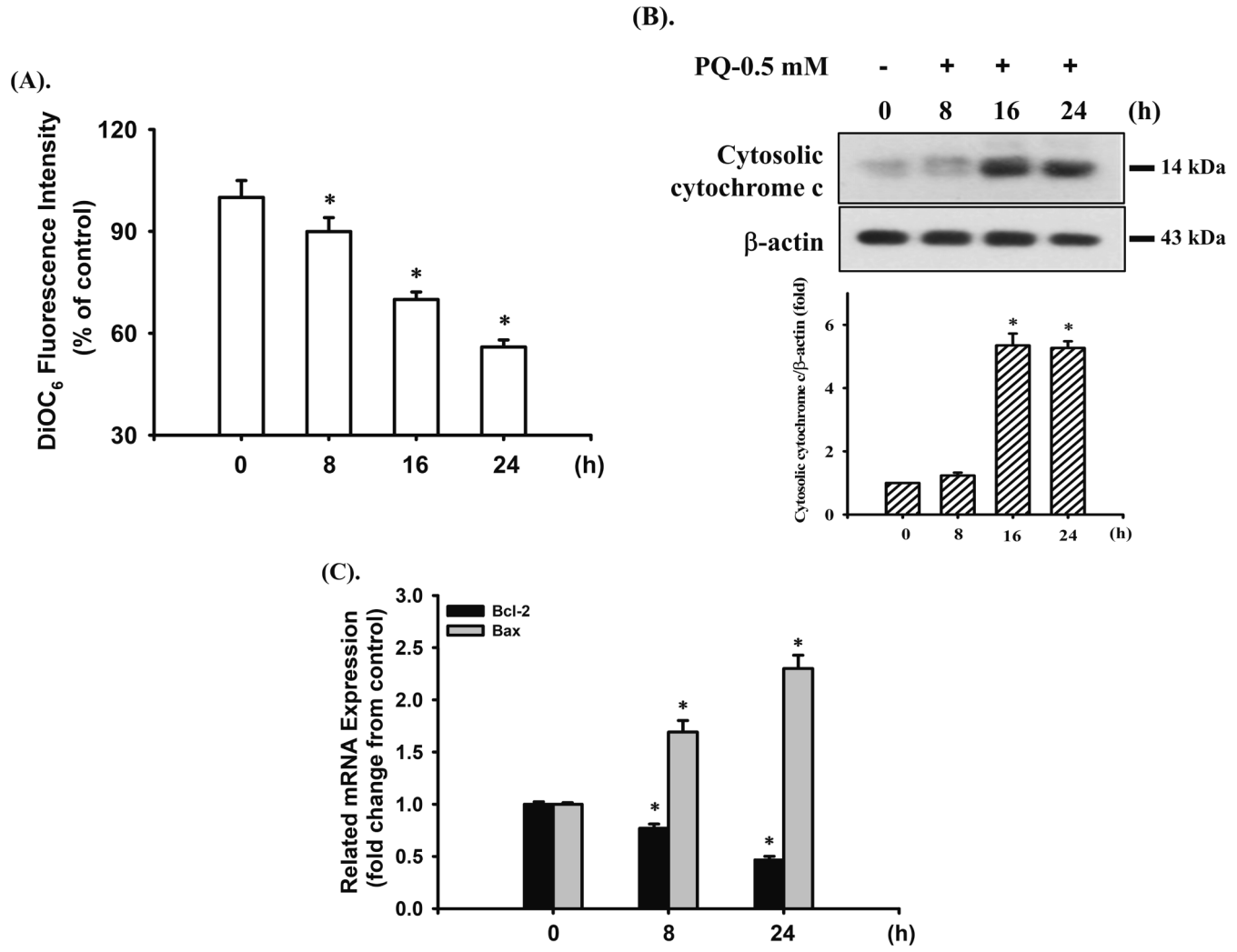

Fig. 2. PQ-induced mitochondrial dysfunction in H4IIE cells. Cells were treated with PQ (0.5 mM) for 8–24 h, and (A) loss of mitochondrial membrane potential (MMP) was determined by flow cytometry; (B) cytosolic cytochrome *c* release was analyzed by western blot analysis; and (C) the expressions of anti-apoptotic (*Bcl-2*) and pro-apoptotic (*Bax*) genes were analyzed by real-time quantitative RT-PCR. Data in A and C are presented as mean ± S.E. for six independent experiments with triplicate determination. *$p < 0.05$ compared to vehicle control. Results shown in B are representative images of at least three independent experiments, and β-actin is used as an internal control.

3.3. JNK and ERK1/2 signals play important roles in PQ-induced H4IIE apoptosis

To ascertain whether the activation of MAPKs was involved in PQ-induced H4IIE cell cytotoxicity and apoptosis, the phosphorylation of MAPKs proteins was examined by western blot analysis. As shown in Fig. 3, treatment of H4IIE cells with PQ (0.5 mM) for 0.5–1.5 h significantly increased the phosphorylation levels of JNK and ERK1/2 proteins, but not p38-MAPK. Pretreatment with specific inhibitors of JNK (SP600125) and ERK1/2 (PD98059) effectively attenuated the decrease in the number of viable cells (Fig. 4A), loss of MMP (Fig. 4B), apoptotic responses (including caspase-3 activity induction (Fig. 4C), and cleaved form expression of caspase-3 and -7 proteins (Fig. 4D)). SP600125 and PD98059 significantly inhibited the phosphorylation of JNK1/2 (Fig. 4E) and ERK1/2 (Fig. 4F), respectively. These findings indicate that activation of the JNK and ERK pathways downstream-mediated mitochondria-dependent apoptosis is involved in PQ-induced H4IIE cell death.

3.4. Pq-induced H4IIE cell death via a ROS-dependent apoptotic pathway

Next, we determined whether PQ stimulated ROS generation and its related apoptosis in H4IIE cells. Flow cytometric analysis showed that exposure of H4IIE cells to 0.5 mM PQ for 0.25–2 h triggered a significant increase in the intensity of dichlorofluorescein (DCF) fluorescence (an indicator of ROS formation) in a time-dependent manner (Fig. 5A). Concomitantly, exposure of H4IIE cells to PQ (0.1–2 mM) for 8 h caused substantial intracellular GSH depletion in a dose-dependent manner (Fig. 5B).

Because PQ stimulated ROS, and JNK and ERK activation down-regulated H4IIE cell apoptotic signals, we examined whether there was a relationship between ROS generation and JNK and ERK activation in PQ-induced H4IIE cell death. Pretreatment with NAC (3 mM; an antioxidant and GSH precursor) for 1 h prior to PQ exposure significantly prevented ROS production (Fig. 6A), intracellular GSH depletion (Fig. 6B), cytotoxicity (Fig. 6C), apoptotic responses (Fig. 6D-6E), loss of MMP (Fig. 6F), and phosphorylation of JNK and ERK1/2 proteins (Fig. 6G). However, pretreatment with SP600125 or PD98059 did not prevent PQ-induced ROS production (Fig. 6A). These results indicate that ROS plays an important role in the activation of JNK/ERK signaling-mediated mitochondria-dependent pathway-triggered apoptosis in PQ-induced hepatic cell death.

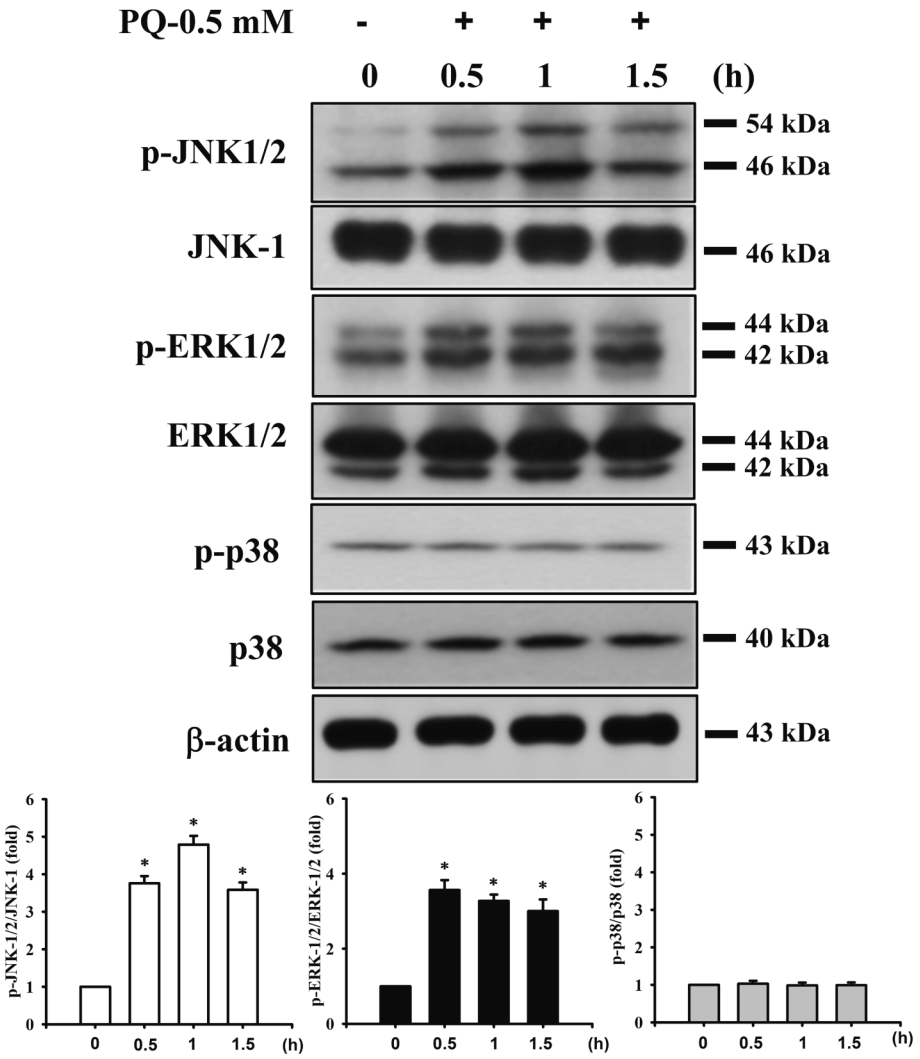

Fig. 3. Effects of PQ on the activation of mitogen-activated protein kinases (MAPKs). H4IIE cells were treated with PQ (0.5 mM) for 0.5–1.5 h, and the phosphorylation of JNK, ERK1/2, and p38-MAPK proteins was analyzed by western blotting. Representative images of at least three independent experiments are shown.

4. Discussion

PQ, one of the commonly used herbicides in agriculture, is an environmental pollutant considered a major health concern for both humans and mammals. It has been reported that PQ poisoning is caused by the accumulation of PQ molecules that trigger the excessive production of ROS, causing oxidative stress injury in cells resulting in multiple organ failure and severe damage (Alizadeh et al., 2022; Chen et al., 2021). The lungs are the primary organs affected; however, PQ can also exert toxic effects on other organs, such as the liver (Fernando et al., 2018; Hong et al., 2000; Takegoshi et al., 1988). The liver is the main site of xenobiotic metabolism and has a high potential for ROS production, which can lead to toxicity (Lattuca et al., 2009). Epidemiological and animal studies have shown that PQ can induce multiple organ injuries (including hepatotoxicity) in mammals after the higher dose and prolonged exposure, accompanied by increased formation of ROS (Almeida et al., 2021; Delirrad et al., 2015; Zhang et al., 2020a). Thus, the liver is regarded as a key target organ for PQ toxicity (El-Boghdady et al., 2017; Fernando et al., 2018). Several studies have shown that exposure to PQ (0.1–1.2 mM) can stimulate neuronal and lung epithelial cells, but not hepatocytes, leading to cytotoxicity and apoptosis, which is mediated by oxidative stress damage-regulated JNK/REK/p38 signaling (Ju et al., 2019; Shen et al., 2017; Sun et al., 2018; Zhang et al., 2019). A study by Zhang et al., (2020a) reported that PQ exposure (0.1–1.0 mM, and EC_{50} ~ 0.5 mM) can induce mitochondrial dysfunction and apoptosis in hepatocytes, triggered by ROS generation. The results from animal experiments also showed the histopathological alterations, abnormalities of biochemical enzymes activity, and apoptosis in the liver tissue after PQ treatment (50–75 mg/kg, i.p.; approximately to 0.2–0.3 mM) (El-Boghdady et al., 2017; Semeniuk et al., 2021). However, the exact mechanisms underlying PQ-induced hepatic cell damage and death have not yet been elucidated. The main findings of the study showed that exposure of hepatocytes to PQ was capable of triggering cytotoxicity (in a concentration-dependent manner (EC_{50} ~ 0.5 mM)), accompanied by mitochondrial dysfunction (loss of MMP and release of cytochrome *c*) and apoptotic responses. More importantly, our results demonstrated that PQ was capable of inducing not only JNK and ERK1/2 signaling activation, but also oxidative stress damage, which downstream-regulated apoptosis in hepatocytes. These findings highlight the involvement of oxidative stress-induced JNK/ERK activation-regulated apoptotic mechanisms in PQ-induced hepatocyte death.

JNK and ERK1/2 are stress-activated members of the MAPK family and are involved in the regulation of cell proliferation, differentiation, survival and apoptosis (Plotnikov et al., 2011). Further, JNK and ERK1/2 have attracted attention as mediators of cell stress responses, as they are involved in the deterioration of mammalian cell function and the regulation of pro-apoptotic/pathological processes of various organ/tissue dysfunctions and injuries, including the liver (Huang et al., 2021;

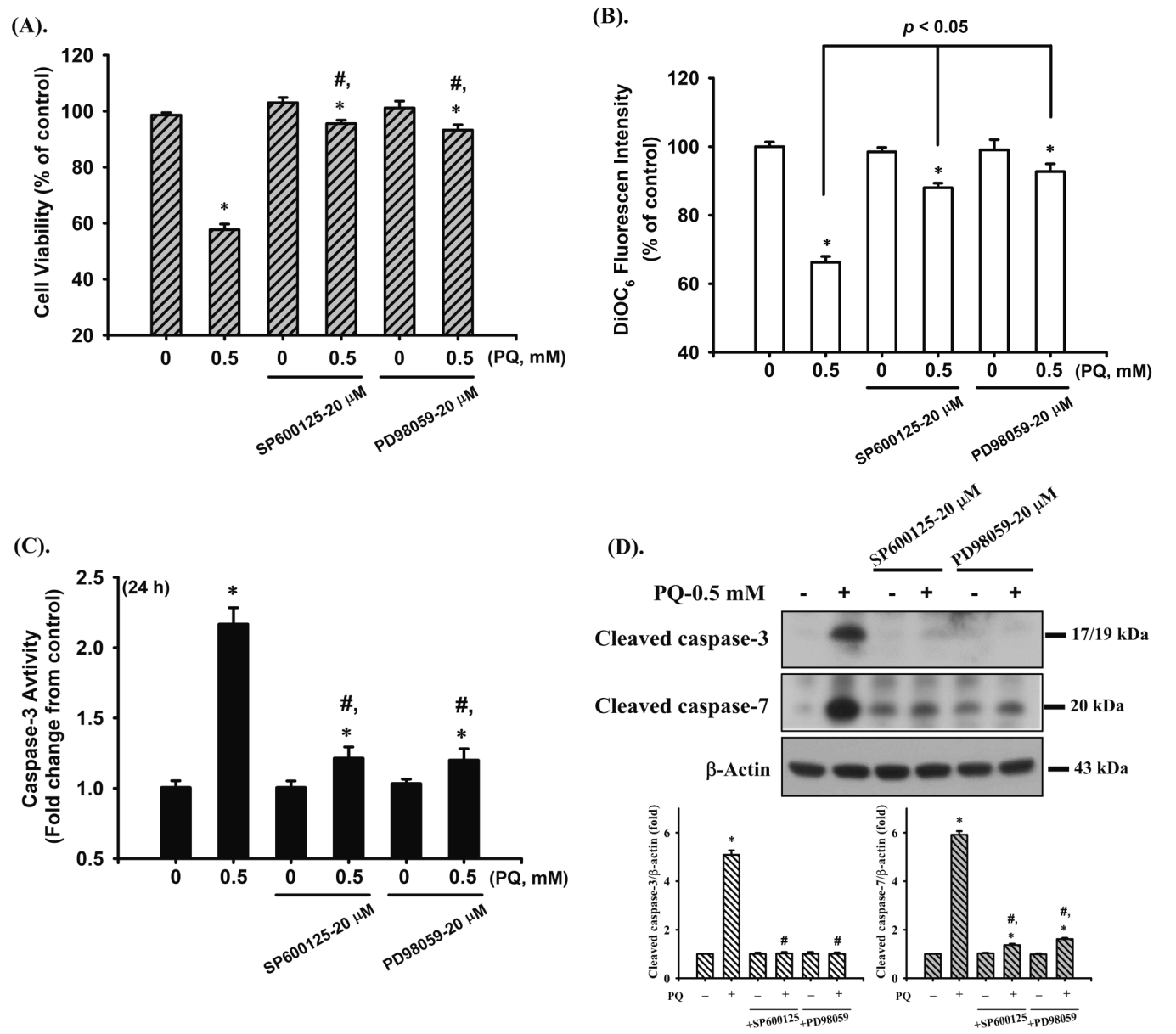

Fig. 4. JNK- and ERK-mediated pathways are critical in PQ-induced apoptosis of H4IIE cells. Cells were treated with a specific JNK inhibitor (SP600125, 20 μM) or ERK1/2 inhibitor (PD98059, 20 μM) for 1 h prior to PQ (0.5 mM) treatment, and then (A) cell viability was determined by MTT assay (for 24 h); (B) loss of MMP was analyzed by flow cytometry (for 24 h); (C) caspase-3 activity was determined using the CaspACE^{TM} fluorometric activity assay kit (for 24 h); (D) protein expressions of caspase-3 and -7 (for 24 h); and (E and F) the phosphorylated levels of JNK and ERK1/2 proteins (for 1 h) were analyzed using western blot analysis. Data in A-C are presented as mean ± S.E. for six independent experiments with triplicate determination. *$p < 0.05$ compared to vehicle control. #$p < 0.05$ compared to PQ treatment alone. Results shown in D-F are representative images of at least three independent experiments.

2019; Lu and Xu, 2006). Growing evidence indicates that exposure to toxic chemicals (such as carbon tetrachloride (CCl_4) or acetaminophen) can induce acute liver injury, leading to hepatocyte death, which is correlated with the JNK/ERK activation-regulated apoptosis pathway (Li et al., 2019; Liu et al., 2018). Furthermore, MAPKs sense the cellular redox status, which can be induced or mediated by ROS activation pathways, indicating that MAPKs are common targets for ROS (Son et al., 2011). The results from *in vitro* experimental paradigms have shown that the JNK/ERK signaling pathway is involved in toxic stimuli-induced hepatotoxicity, which is accompanied by oxidative stress interactions, resulting in apoptosis and pathophysiological injuries (Li et al., 2020; Yang et al., 2018). Some studies have reported that PQ exposure can cause cytotoxicity, and increase ERK signal activation, leading to apoptosis in various cell types, including microglial, embryonic fibroblast, neuroblastoma, and pulmonary alveolar epithelial cells (Ju et al., 2019; Miller et al., 2007; Seo et al., 2014; Zhang et al., 2019). Shen et al. (2017) and Yang et al. (2009) also observed that the JNK inhibitor SP600125 effectively reduced JNK protein phosphorylation and downregulated cleaved caspase-3 protein levels and apoptotic DNA damage, which improved apoptosis in neuroblastoma and pulmonary alveolar epithelial cells and lung tissue injury after PQ poisoning. Although studies have indicated that PQ exposure can induce hepatotoxicity in *in vivo* and in vitro systems by causing apoptosis, abnormalities in histopathological changes, and serum liver enzyme activities (Almeida et al., 2021; Atashpour et al., 2017; El-Boghdady et al., 2017; Kheiripour et al., 2021), the toxicological effects and possible mechanisms of JNK/ERK signaling in PQ-induced hepatotoxicity remain unknown. In the present study, our results found that the treatment of

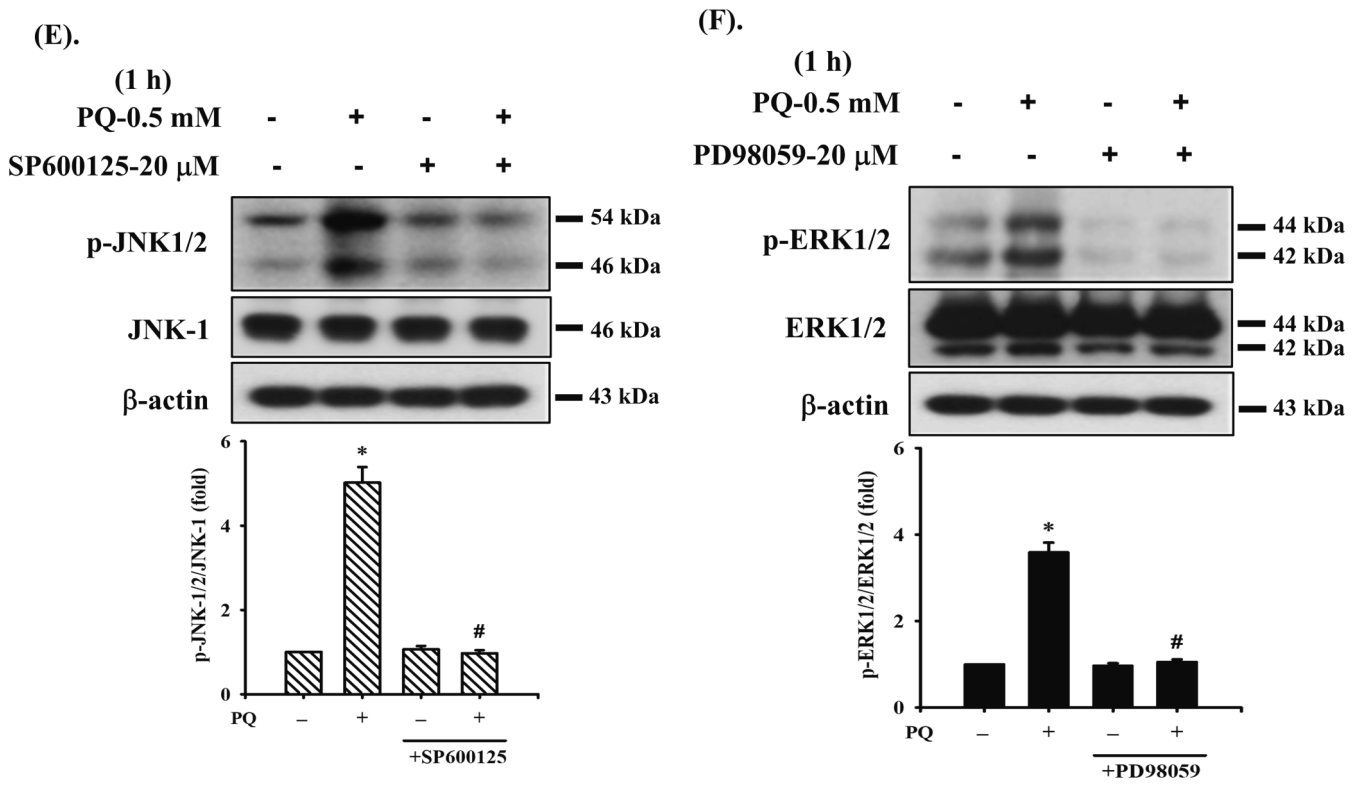

Fig. 4. (*continued*).

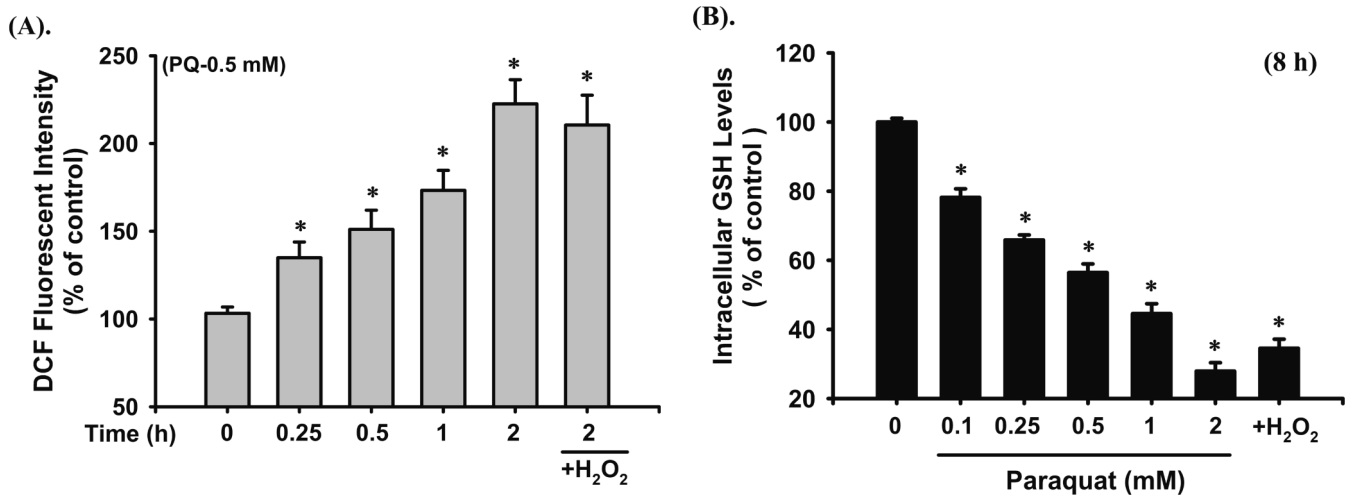

Fig. 5. Effects of PQ on oxidative stress damage in H4IIE cells. Cells were treated with PQ for various time intervals, and (A) ROS generation was determined by flow cytometry (0.25–2 h); (B) the intracellular glutathione (GSH) levels (for 8 h) were detected using a sensitive mBCL fluorescent probe. All data are presented as mean ± S.E. for six independent experiments with triplicate determination. *$p < 0.05$ compared to vehicle control·H_2O_2 (200 μM) was used as a positive control.

hepatic cells with PQ significantly increased the phosphorylated levels of JNK and ERK1/2 proteins, but not that of p38-MAPK. Pretreatment of H4IIE cells with the JNK inhibitor SP600125 and ERK1/2 inhibitor PD98059, respectively, not only effectively blocked the phosphorylation of JNK and ERK1/2, but also markedly abrogated cytotoxicity, loss of MMP, and apoptotic responses in PQ-treated hepatic cells. These results imply that JNK/ERK activation downstream regulated mitochondria-dependent apoptosis plays a crucial role in PQ-induced hepatic cell death.

ROS, which elicit oxidative stress, can affect a variety of patho-physiological processes and induce undesirable biological reactions, such as apoptosis (Redza-Dutordoir and Averill-Bates, 2016). In mammals, the liver is a most important organ because of its metabolic and detoxifying activities, which play a key role in the metabolism of GSH (the main endogenous antioxidant), and that is particularly susceptible to oxidative stress. It is well known that toxic insults are further transformed and metabolized after being absorbed by the body, leading to the overproduction of free radicals (to elicit oxidative stress), resulting in hepatocyte oxidative damage and death (Parvez et al., 2018). Moreover, NADPH oxidases have been discovered in the liver and are sources of ROS that play critical roles in the progression of hepatic diseases (Liang et al., 2016). Nonetheless, PQ is very poisonous to both humans and animals because of its toxicological characteristics of inducing ROS (Chen et al., 2015; Muthu et al., 2015). PQ can be

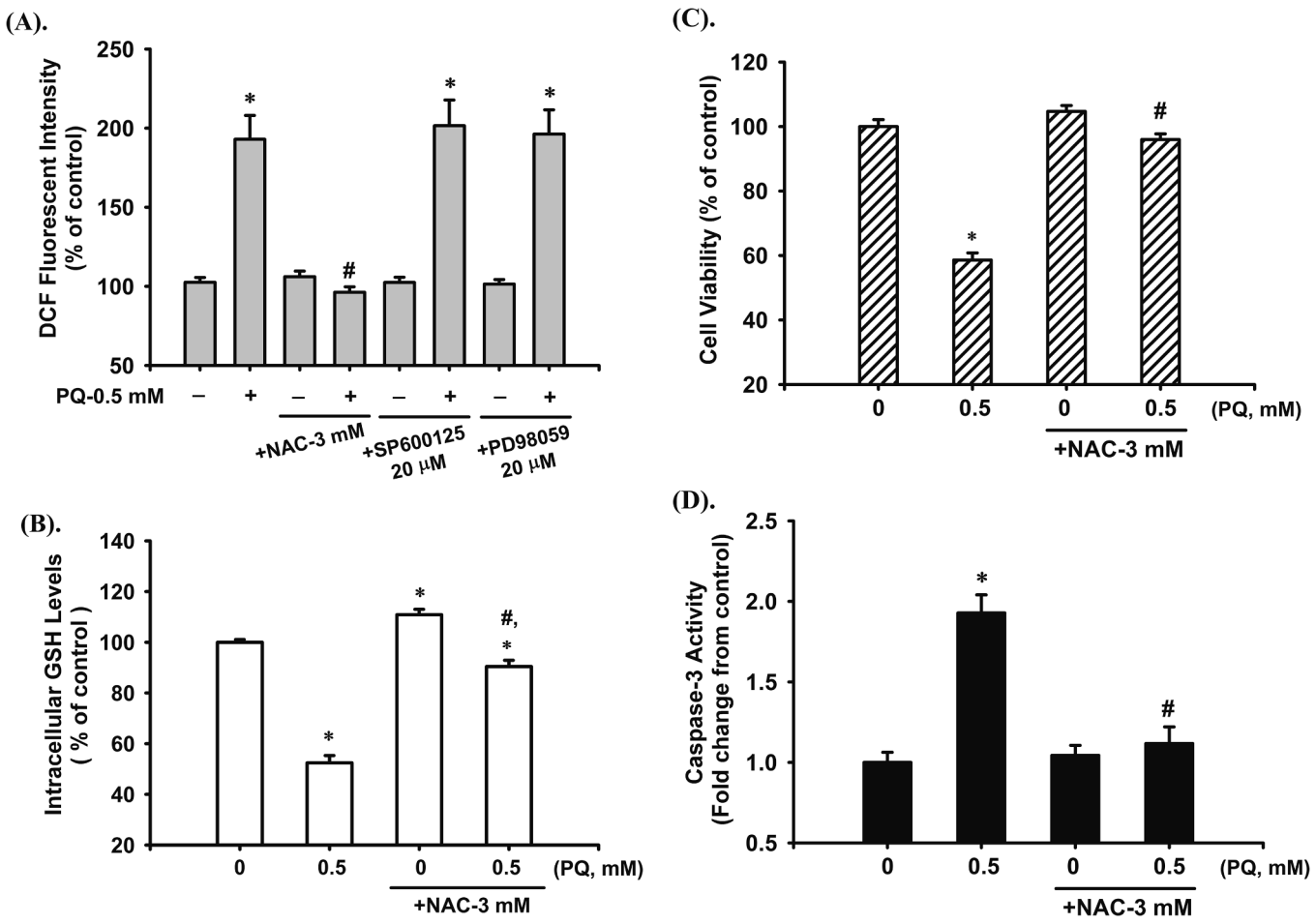

Fig. 6. ROS-mediated pathway plays a crucial role in PQ-induced H4IIE cell apoptosis. H4IIE cells were treated with PQ (0.5 mM) for various time intervals in the absence or presence of NAC (3 mM), SP600125 (20 μM) or PD98059 (20 μM), respectively, and (A) ROS production was determined by flow cytometry (for 2 h); (B) intracellular glutathione (GSH) levels were detected using a sensitive mBCL fluorescent probe (for 8 h); (C) cell viability was detected by MTT assay (for 24 h); (D) caspase-3 activity was determined using the CaspACE^{TM} fluorometric activity assay kit (for 24 h); (E) the cleavage forms of caspase-3 and -7 were examined by western blotting (for 24 h); (F) loss of MMP was detected using flow cytometry (for 24 h); and (G) the protein expressions of phosphorylated JNK and ERK1/2 were examined by western blot analysis (for 1 h). Data in A-D and F are presented as mean ± S.E. for six independent experiments with triplicate determination. *$p < 0.05$ compared to vehicle control. #$p < 0.05$ compared to PQ treatment alone. Results shown in E and G are representative images of at least three independent experiments.

converted to paraquat radicals by NADPH oxidase, which then inhibit the synthesis of NADPH, ultimately producing ROS (such as hydroxyl radicals (OH^-) and hydrogen peroxide (H_2O_2)). These undesirable reactions result in oxidative stress and at subsequently compromised antioxidant defense system (such as the depletion of endogenous natural GSH), which is accompanied by various types of cell damage, especially in the hepatocytes (El-Boghdady et al., 2017). PQ-induced hepatotoxicity is primarily mediated by ROS overproduction, which induces oxidative stress, a vital incentive for organelle dysfunction and apoptosis (Atashpour et al., 2017; Kheiripour et al., 2021; Zeinvand-Lorestani et al., 2018; Zhang et al., 2020a). Several studies in *in vitro* and *in vivo* experimental systems have demonstrated severe GSH depletion under PQ-induced oxidative stress, resulting in hepatocyte dysfunction and liver failure (Almeida et al., 2021; El-Boghdady et al., 2017; Ijaz et al., 2024; Zhang et al., 2020b). Zhang et al., (2020a) also highlighted that PQ exposure can induce marked cytotoxic responses in hepatocytes, including a decrease in cell viability and an increase in the apoptosis rate, mitochondrial dysfunction, and intracellular ROS production. However, the possible mechanism, especially in detailed analysis of the regulatory role of oxidative stress-linked JNK/ERK signaling, in PQ-induced hepatocyte apoptosis, remains to be clarified. The results of the current study showed that exposure of H4IIE cells to PQ resulted in significant cytotoxicity and JNK/ERK activation (the phosphorylation of JNK and ERK1/2 proteins) downstream-regulated mitochondrial dysfunction, leading to apoptosis, which was accompanied by the induction of intracellular ROS generation and GSH depletion. Pretreatment of the cells with the antioxidant NAC (a GSH precursor that results in increased GSH synthesis, leading to protection against oxidative stress-induced damage) attenuated the decrease in cell viability, loss of MMP, apoptotic responses, and intracellular GSH depletion, and JNK and ERK1/2 phosphorylation in PQ-treated H4IIE cells. Increased ROS production in PQ-treated H4IIE cells was effectively prevented by NAC but not a JNK inhibitor (SP600125) or ERK inhibitor (PD98059). These findings suggest that oxidative stress plays a critical role in PQ-induced cytotoxicity, causing JNK/ERK activation downstream-regulated mitochondria-dependent apoptosis, subsequently contributing to hepatocyte death.

5. Conclusions

Overall, the present findings show that PQ is capable of inducing toxicological effects and oxidative stress damage causing hepatocyte

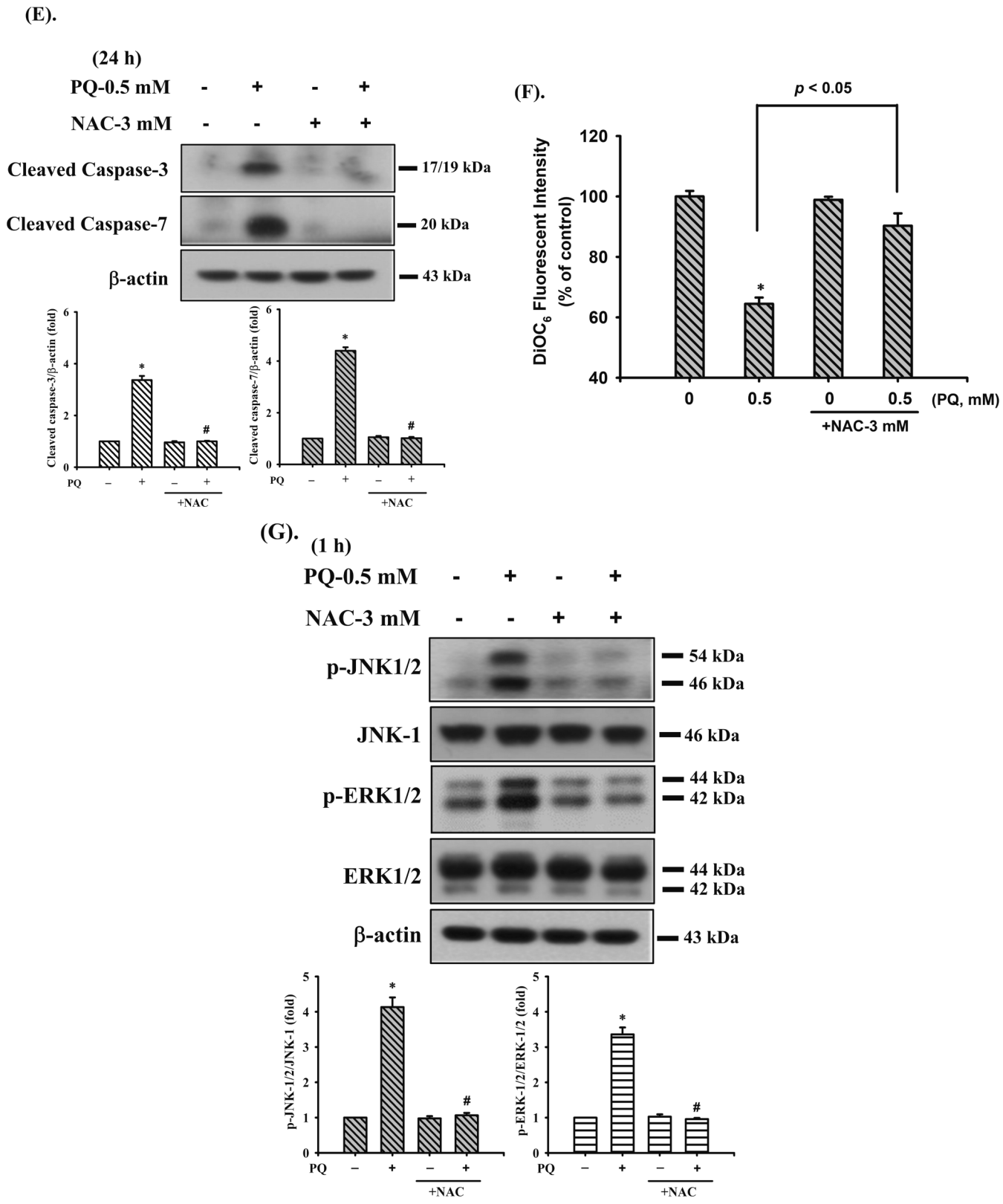

Fig. 6. (*continued*).

apoptosis. Furthermore, as shown in Fig. 7, our findings elucidate that PQ triggers hepatocyte apoptosis through the JNK/ERK activation-regulated downstream mitochondria-dependent pathway. ROS-activated JNK/ERK signal is identified as a key axis in PQ-induced hepatotoxicity, thus further clarifying the mechanisms underlying PQ-induced hepatocyte apoptosis. These observations provide additional evidence that NAC is an effective antidote against PQ-induced hepatotoxicity.

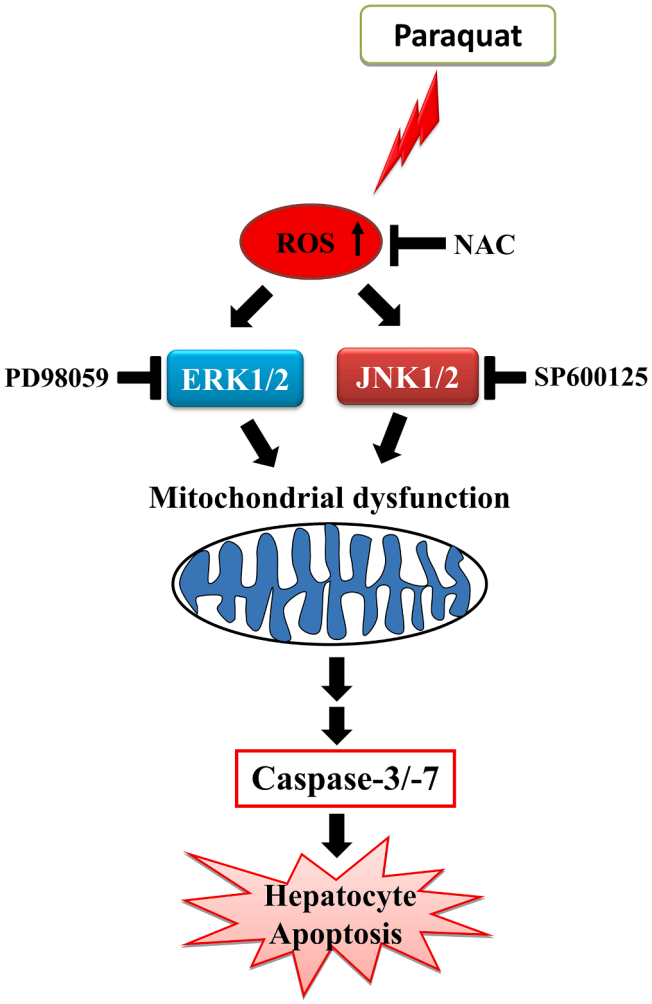

Fig. 7. Schematic diagram of the signaling pathways involved in PQ-induced hepatocyte apoptosis. Proposed models depict that PQ causes hepatocyte death through oxidative stress-induced JNK/ERK activation downstream regulated mitochondria-dependent apoptotic signaling cascades.

CRediT authorship contribution statement

Kuan-I Lee, Kai-Min Fang, and Chun-Ying Kuo: Conceptualization, Investigation, Methodology, Data curation, Project administration, Writing-original draft. Chun-Fa Huang, Shing-Hwa Liu, and Jui-Ming Liu: Methodology, Validation, Formal analysis. Chun-Fa Huang, Wei-Cheng Lai, and Kai-Chih Chang: Visualization, Software, Resources. Kuan-I Lee, Chin-Chuan Su and Ya-Wen Chen: Funding acquisition. Chin-Chuan Su and Ya-Wen Chen: Conceptualization, Investigation, Supervision, Project administration, Writing-review & editing.

Declaration of competing interest

The authors declare that they have no known competing financial interests or personal relationships that could have appeared to influence the work reported in this paper.

Data availability

Data will be made available on request.

Acknowledgments

This work was supported by grants from the Taichung Tzu Chi Hospital, Buddhist Tzu Chi Medical Foundation, Taichung, Taiwan (TTCRD 112-01), the Changhua Christian Hospital, Changhua, Taiwan (112-CCH-IRP-034), and the China Medical University, Taichung, Taiwan (CMU112-S-19).

References

Alizadeh, S., Anani-Sarab, G., Amiri, H., Hashemi, M., 2022. Paraquat induced oxidative stress, DNA damage, and cytotoxicity in lymphocytes. Heliyon 8, e09895.

Almeida, L.L., Pitombeira, G., Teixeira, A.A.C., Teixeira, V.W., Silva Junior, V.A., Vieira Filho, L.D., Evencio Neto, J., 2021. Protective effect of melatonin against herbicides-induced hepatotoxicity in rats. Toxicol. Res. (camb) 10, 1–10. https://doi.org/10.1093/toxres/tfaa087.

Alural, B., Ozerdem, A., Allmer, J., Genc, K., Genc, S., 2015. Lithium protects against paraquat neurotoxicity by NRF2 activation and miR-34a inhibition in SH-SY5Y cells. Front. Cell. Neurosci. 9, 209. https://doi.org/10.3389/fncel.2015.00209.

Atashpour, S., Kargar Jahromi, H., Kargar Jahromi, Z., Zarei, S., 2017. Antioxidant effects of aqueous extract of Salep on Paraquat-induced rat liver injury. World J. Hepatol. 9, 209–216. https://doi.org/10.4254/wjh.v9.i4.209.

Awadalla, E.A., 2012. Efficacy of vitamin C against liver and kidney damage induced by paraquat toxicity. Exp. Toxicol. Pathol. 64, 431–434. https://doi.org/10.1016/j.etp.2010.10.009.

Cantor, A., Young-Holt, B., 2002. Pesticide-related symptoms among farm workers in rural Honduras. Int. J. Occup. Environ. Health 8, 41–45. https://doi.org/10.1179/oeh.2002.8.1.41.

Chen, J.L., Dai, L., Zhang, P., Chen, W., Cai, G.S., Qi, X.W., Hu, M.Z., Du, B., Pang, Q.F., 2015. Methylene blue attenuates acute liver injury induced by paraquat in rats. Int. Immunopharmacol. 28, 808–812. https://doi.org/10.1016/j.intimp.2015.04.044.

Chen, J., Su, Y., Lin, F., Iqbal, M., Mehmood, K., Zhang, H., Shi, D., 2021. Effect of paraquat on cytotoxicity involved in oxidative stress and inflammatory reaction: A review of mechanisms and ecological implications. Ecotoxicolo. Environ. Saf. 224, 112711 https://doi.org/10.1016/j.ecoenv.2021.112711.

Dalvie, M.A., White, N., Raine, R., Myers, J.E., London, L., Thompson, M., Christiani, D. C., 1999. Long-term respiratory health effects of the herbicide, paraquat, among workers in the Western Cape. Occup. Environ. Med. 56, 391–396. https://doi.org/10.1136/oem.56.6.391.

Delirrad, M., Majidi, M., Boushehri, B., 2015. Clinical features and prognosis of paraquat poisoning: a review of 41 cases. Int. J. Clin. Exp. Med. 8, 8122–8128.

Deveci, E., Guven, K., Bashan, M., Onen, A., de Pomerai, D., 1999. The accumulation and histological effects of organometallic fungicides propineb and maneb in the livers of pregnant rats and their offspring. J. Toxicol. Sci. 24, 79–85.

Dinh, C.T., Haake, S., Chen, S., Hoang, K., Nong, E., Eshraghi, A.A., Balkany, T.J., Van De Water, T.R., 2008. Dexamethasone protects organ of corti explants against tumor necrosis factor-alpha–induced loss of auditory hair cells and alters the expression levels of apoptosis-related genes. Neuroscience 157, 405–413. https://doi.org/10.1016/j.neuroscience.2008.09.012.

El-Boghdady, N.A., Abdeltawab, N.F., Nooh, M.M., 2017. Resveratrol and Montelukast Alleviate Paraquat-Induced Hepatic Injury in Mice: Modulation of Oxidative Stress, Inflammation, and Apoptosis. Oxid. Med. Cell. Longev. 2017, 9396425. https://doi.org/10.1155/2017/9396425.

Fernando, M., Camilo, M., Orlando, P., 2018. Paraquat intoxication as a cause of multiple organ failure: report of a case and review of the literature. MOJ Toxicol. 4, 247–253. https://doi.org/10.15406/mojt.2018.04.00108.

Fu, S.C., Liu, J.M., Lee, K.I., Tang, F.C., Fang, K.M., Yang, C.Y., Su, C.C., Chen, H.H., Hsu, R.J., Chen, Y.W., 2020. Cr(VI) induces ROS-mediated mitochondrial-dependent apoptosis in neuronal cells via the activation of Akt/ERK/AMPK signaling pathway. Toxicol. in Vitro 65, 104795. https://doi.org/10.1016/j.tiv.2020.104795.

Hong, S.Y., Yang, D.H., Hwang, K.Y., 2000. Associations between laboratory parameters and outcome of paraquat poisoning. Toxicol. Lett. 118, 53–59. https://doi.org/10.1016/s0378-4274(00)00264-2.

Huang, C.C., Kuo, C.Y., Yang, C.Y., Liu, J.M., Hsu, R.J., Lee, K.I., Su, C.C., Wu, C.C., Lin, C.T., Liu, S.H., Huang, C.F., 2019. Cadmium exposure induces pancreatic beta-cell death via a Ca(2+)-triggered JNK/CHOP-related apoptotic signaling pathway. Toxicology 425, 152252. https://doi.org/10.1016/j.tox.2019.152252.

Huang, C.F., Yang, C.Y., Tsai, J.R., Wu, C.T., Liu, S.H., Lan, K.C., 2018. Low-dose tributyltin exposure induces an oxidative stress-triggered JNK-related pancreatic beta-cell apoptosis and a reversible hypoinsulinemic hyperglycemia in mice. Sci. Rep. 8, 5734. https://doi.org/10.1038/s41598-018-24076-w.

Huang, C.F., Liu, S.H., Su, C.C., Fang, K.M., Yen, C.C., Yang, C.Y., Tang, F.C., Liu, J.M., Wu, C.C., Lee, K.I., Chen, Y.W., 2021. Roles of ERK/Akt signals in mitochondria-dependent and endoplasmic reticulum stress-triggered neuronal cell apoptosis induced by 4-methyl-2,4-bis(4-hydroxyphenyl)pent-1-ene, a major active metabolite of bisphenol A. Toxicology 455, 152764. https://doi.org/10.1016/j.tox.2021.152764.

Ijaz, M.U., Ghafoor, N., Hayat, M.F., Almutairi, B.O., Atique, U., 2024. Amentoflavone mediated hepatoprotection to counteract paraquat instigated hepatotoxicity via modulating Nrf2/keap1 pathway: A biochemical, inflammatory, apoptotic and histopathological study. Pestic. Biochem. Physiol. 198, 105715 https://doi.org/10.1016/j.pestbp.2023.105715.

Isha, I.T., Alam, Z., Shaha, B.K., Bari, M.S., Bari, M.Z.J., Chowdhury, F.R., 2018. Paraquat induced acute kidney injury and lung fibrosis: a case report from Bangladesh. BMC Res. Notes 11, 344. https://doi.org/10.1186/s13104-018-3425-3.

Jimenez Del Rio, M., Velez-Pardo, C., 2008. Paraquat induces apoptosis in human lymphocytes: Protective and rescue effects of glucose, cannabinoids and insulin-like

growth factor-1. Growth Factors 26, 49–60. https://doi.org/10.1080/08977190801984205.
Ju, D.T., Sivalingam, K., Kuo, W.W., Ho, T.J., Chang, R.L., Chung, L.C., Day, C.H., Viswanadha, V.P., Liao, P.H., Huang, C.Y., 2019. Effect of Vasicinone against Paraquat-Induced MAPK/p53-Mediated Apoptosis via the IGF-1R/PI3K/AKT Pathway in a Parkinson's Disease-Associated SH-SY5Y Cell Model. Nutrients 11, 1655. https://doi.org/10.3390/nu11071655.
Kheiripour, N., Plarak, A., Heshmati, A., Asl, S.S., Mehri, F., Ebadollahi-Natanzi, A., Ranjbar, A., Hosseini, A., 2021. Evaluation of the hepatoprotective effects of curcumin and nanocurcumin against paraquat-induced liver injury in rats: Modulation of oxidative stress and Nrf2 pathway. J. Biochem. Mol. Toxicol. 35, e22739. https://doi.org/10.1002/jbt.22739.
Lattuca, M.E., Malanga, G., Aguilar Hurtado, C., Perez, A.F., Calvo, J., Puntarulo, S., 2009. Main features of the oxidative metabolism in gills and liver of Odontesthes nigricans Richardson (Pisces, Atherinopsidae). Comp. Biochem. Physiol. B Biochem. Mol. Biol. 154, 406–411. https://doi.org/10.1016/j.cbpb.2009.08.004.
Li, Y., Ding, H., Liu, L., Song, Y., Du, X., Feng, S., Wang, X., Li, X., Wang, Z., Li, X., Li, J., Wu, J., Liu, G., 2020. Non-esterified Fatty Acid Induce Dairy Cow Hepatocytes Apoptosis via the Mitochondria-Mediated ROS-JNK/ERK Signaling Pathway. Front. Cell Dev. Biol. 8, 245. https://doi.org/10.3389/fcell.2020.00245.
Li, X., Lin, J., Lin, Y., Huang, Z., Pan, Y., Cui, P., Yu, C., Cai, C., Xia, J., 2019. Hydrogen sulfide protects against acetaminophen-induced acute liver injury by inhibiting apoptosis via the JNK/MAPK signaling pathway. J. Cell. Biochem. 120, 4385–4397. https://doi.org/10.1002/jcb.27724.
Li, S., Tan, H.Y., Wang, N., Zhang, Z.J., Lao, L., Wong, C.W., Feng, Y., 2015. The Role of Oxidative Stress and Antioxidants in Liver Diseases. Int. J. Mol. Sci. 16, 26087–26124. https://doi.org/10.3390/ijms161125942.
Liang, S., Kisseleva, T., Brenner, D.A., 2016. The Role of NADPH Oxidases (NOXs) in Liver Fibrosis and the Activation of Myofibroblasts. Front. Physiol. 7, 17. https://doi.org/10.3389/fphys.2016.00017.
Liu, Y., Wen, P.H., Zhang, X.X., Dai, Y., He, Q., 2018. Breviscapine ameliorates CCl4 induced liver injury in mice through inhibiting inflammatory apoptotic response and ROS generation. Int. J. Mol. Med. 42, 755–768. https://doi.org/10.3892/ijmm.2018.3651.
Liu, Y., Luo, X.J., Li, G.Q., Wei, L.Q., Yu, X., Li, Y.M., 2019. Increased 90-Day Mortality in Spontaneously Breathing Patients With Paraquat Poisoning. In Addition to Disease Severity, Lung Strain May Play a Role. Crit. Care Med. 47, 219–228. https://doi.org/10.1097/CCM.0000000000003518.
Lu, T.H., Hsieh, S.Y., Yen, C.C., Wu, H.C., Chen, K.L., Hung, D.Z., Chen, C.C., Su, Y.C., Chen, Y.W., Liu, S.H., Huang, C.F., 2011. Involvement of oxidative stress-mediated ERK1/2 and p38 activation regulated mitochondria-dependent apoptotic signals in methylmercury-induced neuronal cell injury. Toxicol. Lett. 204, 71–80. https://doi.org/10.1016/j.toxlet.2011.04.013.
Lu, Z., Xu, S., 2006. ERK1/2 MAP kinases in cell survival and apoptosis. IUBMB Life 58, 621–631. https://doi.org/10.1080/15216540600957438.
Miller, R.L., Sun, G.Y., Sun, A.Y., 2007. Cytotoxicity of paraquat in microglial cells: Involvement of PKCδ- and ERK1/2-dependent NADPH oxidase. Brain Res. 1167, 129–139. https://doi.org/10.1016/j.brainres.2007.06.046.
Moustakas, M., Malea, P., Zafeirakoglou, A., Sperdouli, I., 2016. Photochemical changes and oxidative damage in the aquatic macrophyte Cymodocea nodosa exposed to paraquat-induced oxidative stress. Pestic. Biochem. Physiol. 126, 28–34. https://doi.org/10.1016/j.pestbp.2015.07.003.
Muthu, V., Das, A., Bal, A., Agarwal, R., 2015. Severe cholestasis and hepatic dysfunction in a case of fatal paraquat poisoning. Clin. Res. Hepatol. Gastroenterol. 39, e7–e9. https://doi.org/10.1016/j.clinre.2014.07.013.
Parvez, M.K., Arbab, A.H., Al-Dosari, M.S., Al-Rehaily, A.J., Alam, P., Ibrahim, K.E., Alsaid, M.S., Rafatullah, S., 2018. Protective effect of Atriplex suberecta extract against oxidative and apoptotic hepatotoxicity. Exp. Ther. Med. 15, 3883–3891. https://doi.org/10.3892/etm.2018.5919.
Pfaffl, M.W., Horgan, G.W., Dempfle, L., 2002. Relative expression software tool (REST) for group-wise comparison and statistical analysis of relative expression results in real-time PCR. Nucleic Acids Research 30, e36.
Plotnikov, A., Zehorai, E., Procaccia, S., Seger, R., 2011. The MAPK cascades: Signaling components, nuclear roles and mechanisms of nuclear translocation. Biochim. Biophys. Acta.- Mol. Cell Res. 1813, 1619–1633. https://doi.org/10.1016/j.bbamcr.2010.12.012.
Redza-Dutordoir, M., Averill-Bates, D.A., 2016. Activation of apoptosis signalling pathways by reactive oxygen species. Biochim. Biophys. Acta 1863, 2977–2992. https://doi.org/10.1016/j.bbamcr.2016.09.012.
Semeniuk, M., Ceré, L.I., Ciriaci, N., Bucci-Muñoz, M., Quiroga, A.D., Luquita, M.G., Roma, S., Catania, V.A., Mottino, A.D., Rigalli, J.P., Ruiz, M.L., 2021. Protective effect of genistein pre-treatment on paraquat hepatotoxicity in rats. Toxicol. Appl. Pharmacol. 426, 115636 https://doi.org/10.1016/j.taap.2021.115636.
Seo, H.J., Choi, S.J., Lee, J.H., 2014. Paraquat Induces Apoptosis through Cytochrome C Release and ERK Activation. Biomol. Ther (seoul) 22, 503–509. https://doi.org/10.4062/biomolther.2014.115.
Sharifi-Rigi, A., Heidarian, E., Amini, S.A., 2019. Protective and anti-inflammatory effects of hydroalcoholic leaf extract of Origanum vulgare on oxidative stress, TNF-alpha gene expression and liver histological changes in paraquat-induced hepatotoxicity in rats. Arch Physiol. Biochem. 125, 56–63. https://doi.org/10.1080/13813455.2018.1437186.
Shen, H., Wu, N., Wang, Y., Han, X., Zheng, Q., Cai, X., Zhang, H., Zhao, M., 2017. JNK Inhibitor SP600125 Attenuates Paraquat-Induced Acute Lung Injury: an In Vivo and In Vitro Study. Inflammation 40, 1319–1330. https://doi.org/10.1007/s10753-017-0575-8.
Shi, Q., Song, X., Fu, J., Su, C., Xia, X., Song, E., Song, Y., 2015. Artificial sweetener neohesperidin dihydrochalcone showed antioxidative, anti-inflammatory and anti-apoptosis effects against paraquat-induced liver injury in mice. Int. Immunopharmacol. 29, 722–729. https://doi.org/10.1016/j.intimp.2015.09.003.
Son, Y., Cheong, Y.K., Kim, N.H., Chung, H.T., Kang, D.G., Pae, H.O., 2011. Mitogen-Activated Protein Kinases and Reactive Oxygen Species: How Can ROS Activate MAPK Pathways? J. Signal. Transduct. 2011, 792639 https://doi.org/10.1155/2011/792639.
Song, Y., Li, N., Gu, J., Fu, S., Peng, Z., Zhao, C., Zhang, Y., Li, X., Wang, Z., Li, X., Liu, G., 2016. beta-Hydroxybutyrate induces bovine hepatocyte apoptosis via an ROS-p38 signaling pathway. J. Dairy. Sci. 99, 9184–9198. https://doi.org/10.3168/jds.2016-11219.
Spangenberg, T., Grahn, H., Schalk, H., Kuck, K., 2012. Paraquatintoxikation. Med. Klin. Intensivmed. Notfmed. 4, 270–274. https://doi.org/10.1007/s00063-011-0074-x.
Sun, Y., Liu, W.Z., Liu, T., Feng, X., Yang, N., Zhou, H.F., 2015. Signaling pathway of MAPK/ERK in cell proliferation, differentiation, migration, senescence and apoptosis. J. Recept. Signal. Transduct. Res. 35, 600–604. https://doi.org/10.3109/10799893.2015.1030412.
Sun, D.Z., Song, C.Q., Xu, Y.M., Wang, R., Liu, W., Liu, Z., Dong, X.S., 2018. Involvement of PINK1/Parkin-mediated mitophagy in paraquat- induced apoptosis in human lung epithelial-like A549 cells. Toxicol. in Vitro 53, 148–159. https://doi.org/10.1016/j.tiv.2018.08.009.
Takegoshi, K., Nakanuma, Y., Ohta, M., Thoyama, T., Okuda, K., Kono, N., 1988. Light and electron microscopic study of the liver in paraquat poisoning. Liver 8, 330–336.
Win, S., Than, T.A., Zhang, J., Oo, C., Min, R.W.M., Kaplowitz, N., 2018. New insights into the role and mechanism of c-Jun-N-terminal kinase signaling in the pathobiology of liver diseases. Hepatology 67, 2013–2024. https://doi.org/10.1002/hep.29689.
Wu, J., Li, Y., Li, X., Wu, T., 2023. Swertiamarin attenuates paraquat-induced pulmonary epithelial-like cell apoptosis via NOX4-mediated regulation of redox and mitochondrial function. Braz. J. Pharm. Sci. 59 https://doi.org/10.1590/s2175-97902023e22476.
Yang, W., Tiffany-Castiglioni, E., Koh, H.C., Son, I.H., 2009. Paraquat activates the IRE1/ASK1/JNK cascade associated with apoptosis in human neuroblastoma SH-SY5Y cells. Toxicol. Lett. 191, 203–210. https://doi.org/10.1016/j.toxlet.2009.08.024.
Yang, C.F., Zhong, Y.J., Ma, Z., Li, L., Shi, L., Chen, L., Li, C., Wu, D., Chen, Q., Li, Y.W., 2018. NOX4/ROS mediate ethanol-induced apoptosis via MAPK signal pathway in L-02 cells. Int. J. Mol. Med. 41, 2306–2316. https://doi.org/10.3892/ijmm.2018.3390.
Zeinvand-Lorestani, H., Nili-Ahmadabadi, A., Balak, F., Hasanzadeh, G., Sabzevari, O., 2018. Protective role of thymoquinone against paraquat-induced hepatotoxicity in mice. Pestic. Biochem. Physiol. 148, 16–21. https://doi.org/10.1016/j.pestbp.2018.03.006.
Zhang, Z.D., Huang, M.Z., Yang, Y.J., Liu, X.W., Qin, Z., Li, S.H., Li, J.Y., 2020a. Aspirin Eugenol Ester Attenuates Paraquat-Induced Hepatotoxicity by Inhibiting Oxidative Stress. Front. Physiol. 11, 582801 https://doi.org/10.3389/fphys.2020.582801.
Zhang, L., Li, Q., Liu, Z., Wang, Y., Zhao, M., 2019. The protective effects of bone mesenchymal stem cells on paraquat-induced acute lung injury via the muc5b and ERK/MAPK signaling pathways. Am. J. Transl. Res. 11, 3707–3721.
Zhang, Z.D., Yang, Y.J., Liu, X.W., Qin, Z., Li, S.H., Li, J.Y., 2020b. The Protective Effect of Aspirin Eugenol Ester on Paraquat-Induced Acute Liver Injury Rats. Front. Med. (lausanne) 7, 589011. https://doi.org/10.3389/fmed.2020.589011.